

DETERMINATION OF SELECTED MECHANICAL PROPERTIES OF  
AGED AL-LI ALLOYS USING NDE METHODS

L. J. H. Brasche, O. Buck, D. C. Jiles, J. D. Snodgrass,  
and D. J. Bracci\*

Center for NDE  
Iowa State University  
Ames, IA 50011

\*Now with McDonnell Douglas Corp.  
St. Louis, MO 63166

INTRODUCTION

Al-Li alloys have the combined advantages of high strength and high modulus in addition to a lower density than typical structural aluminum alloys. This combination of properties could be used to reduce the weight of aircraft by about 10% without loss of structural integrity. The mechanical properties of these alloys strongly depend on the morphology of the precipitates within the matrix. Therefore, quantitative NDE techniques for on-line monitoring of microstructural changes during the production of these alloys is desirable from both a quality and economic standpoint. Correlations between mechanical properties, of interest to the designer, and data, resulting from NDE measurements, are reported. Of particular interest is the detection of the T<sub>1</sub> phase which is detrimental to the fatigue properties of such alloys. The results reveal that the appearance of T<sub>1</sub> can be detected by the combined use of eddy current (or DC conductivity) and hardness measurements. The presence of T<sub>1</sub> was verified by transmission electron microscopy (TEM).

EXPERIMENTAL PROCEDURES

The alloys used in this investigation included an Al-2.2 wt % Li (binary) and Al 2090, provided by Alcoa<sup>[1]</sup>, which has a composition of 2.7% Cu, 2.2% Li, 0.12% Zr, 0.08% Si and 0.12% Fe. Solution heat treatment was carried out at 430 C and 540 C for the binary and Al 2090, respectively. The solution heat treatment was followed by a water quench with a cooling rate of approximately 130 deg C/s (WQ) or an air cool with an average cooling rate of 2 deg C/s (AQ). The samples were then thermally aged at temperatures from 150 to 200 C for 3 to 33 h.

As reported earlier<sup>[2]</sup>, flat specimens were used to determine the eddy current response at 5 kHz, the DC conductivity, both Vickers (DPH) and Meyer hardness (MH), the sound velocity and the acoustic attenuation. The mechanical properties were obtained using standard tensile specimens. The 0.2% offset yield stress,  $\sigma_Y$ , the ultimate tensile strength,  $\sigma_{UTS}$ , the strain hardening exponent,  $n$ , and the strain-to-failure,  $\epsilon_f$ , were determined by means of an Instron screw-driven tensile machine at a strain rate of approximately  $1.6 \times 10^{-4} \text{ s}^{-1}$ .

Transmission electron microscopy (TEM) was performed on selected samples. Thin foils were obtained by double-jet polishing in a solution of 25% nitric acid and 75% methanol at -25 C and 20 V and examined using a JEOL 100 CX operating at 120 kV.

## RESULTS

Standard statistical analysis[3] was used to evaluate correlations between mechanical properties and NDE measurements. Table I lists several of the correlations found thus far. Note that for some correlations a linear relationship exists that describes both the binary and 2090 while in other cases two separate relations are required.

As an example, Fig. 1 shows the statistical analysis results for the correlation between  $\sigma_Y$  (in MPa) and DPH. Note that a linear relation describes both the binary and Al 2090 with a correlation coefficient of  $R = 0.97$ .  $N$  is the number of points used in the analysis and  $S_{yx}$  is the standard deviation. A confidence band of one standard deviation, is shown as the dashed lines. Also note, that the binary alloy data are concentrated at low  $\sigma_Y$  and those for Al 2090 at high  $\sigma_Y$ . In addition to the Al-Li results, data for a 65S aluminum alloy reported by Cahoon et al.[4] in either the strain hardened or age hardened conditions are shown in Fig. 1. This alloy has a composition similar to the Al 6061 structural alloy where the increase in strength is a result of  $Mg_2Si$  precipitates[5]. Note that the 65S age hardened results fall within one standard deviation of the linear regression line for the age hardened Al-Li alloys and the results of the strain hardened material are in close proximity to that line.

Table I. Correlations between mechanical properties and NDE measurements for Al-Li alloys (A: correlation applicable; NA: Correlation not applicable; ?: not established yet).

Material				Correlation	$S_{yx}$	R
Al 2090		Binary				
WQ	AQ	WQ	AQ			
A	A	A	A	$\sigma_Y(MPa) = 3.48DPH - 109.2$	24.2	0.97
A	A	A	A	$\sigma_Y(MPa) = 0.31MH - 51.4$	62.7	0.81
NA	NA	A	A	$\sigma_{UTS}(MPa) = 1.2DPH - 142.9$	9.2	0.78
A	A	NA	NA	$\sigma_{UTS}(MPa) = 2.2DPH - 168.1$	13.8	0.96
A	?	A	?	$\Delta Z = 2.66C + 4.70$	0.05	0.99
A	A	NA	NA	$DPH = 88.3\Delta Z - 541.3$	7.6	0.88
NA	NA	A	A	$DPH = 88.5\Delta Z - 633.2$	6.3	0.93
A	?	?	?	$E(GPa) = 69.09$	0.22	

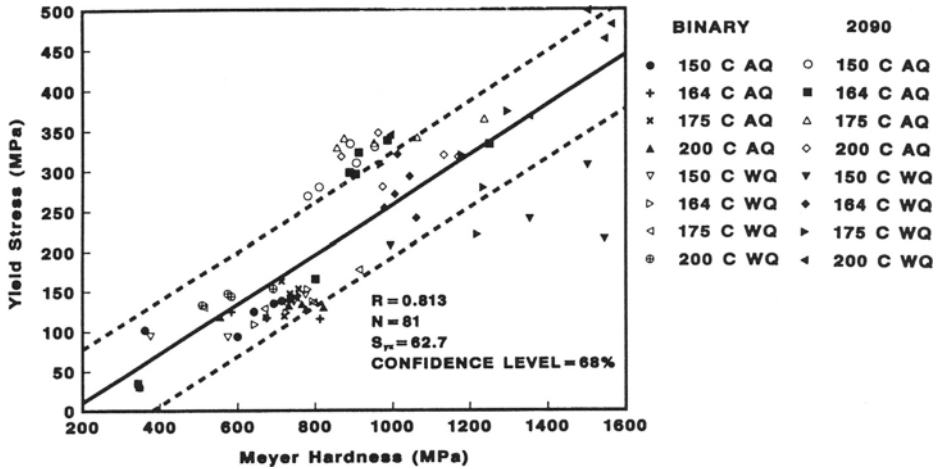


Fig. 1. Yield stress versus Vickers hardness (Al 2090 and binary alloy).

Meyer hardness measurements are useful in that they can be used to predict the strain hardening exponent,  $n$ .<sup>[6]</sup> Dieter<sup>[6]</sup> found that  $K_{IC}$  can be estimated using the relation

$$K_{IC} \sim (2/3 \epsilon_f E \sigma_y n^2)^{1/2}$$

Because Meyer hardness (MH) predicts  $n$  needed in this estimation, MH measurements are presently underway using a 600N load on both the binary and the Al 2090 alloys. First results of a correlation of MH and  $\sigma_y$  are shown in Fig. 2. Note that  $R$  is considerably lower than for  $\sigma_y$  versus DPH which is due to the larger scatter in MH with respect to the DPH measurements.

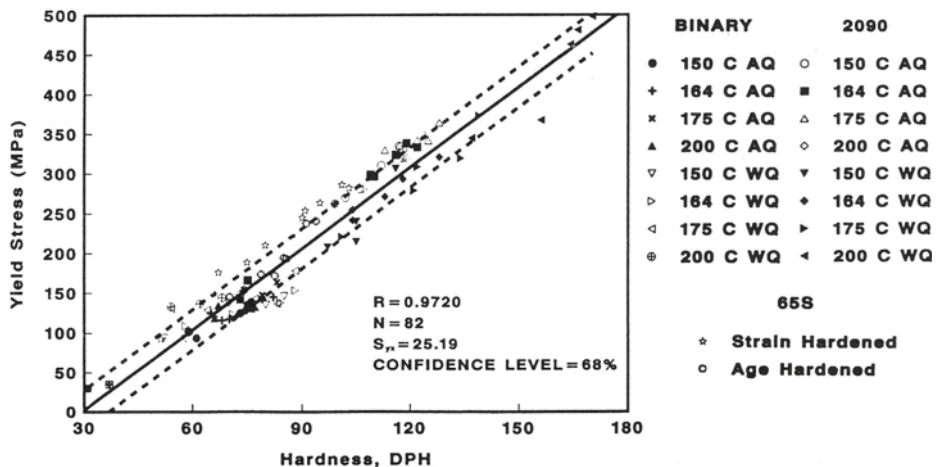


Fig. 2. Yield stress versus Meyer hardness (Al 2090 and binary alloy).

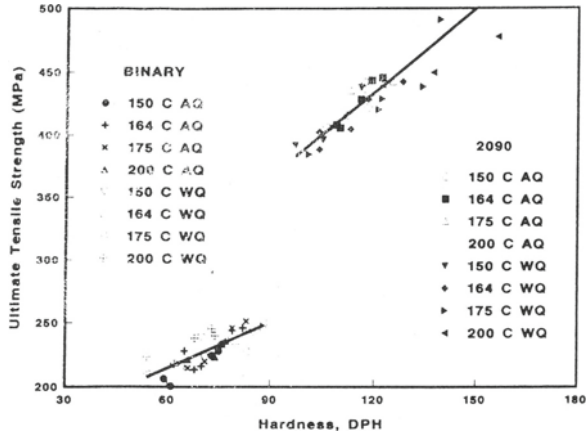


Fig. 3.  $\sigma_{UTS}$  versus Vickers hardness (Al 2090 and binary alloy).

The ultimate tensile stress,  $\sigma_{UTS}$ , was determined from stress-strain curves and correlated with DPH as shown in Fig. 3. The results of the statistical analysis are listed in Table I. Note that the results for the binary alloy are clearly separated from those of Al 2090.

Results of DC conductivity measurements and the eddy current response are shown in Fig. 4 for the water quenched alloys. The data for both alloy systems lie on a single linear regression line which indicates that the eddy current response can be used to predict the DC conductivity or vice versa.

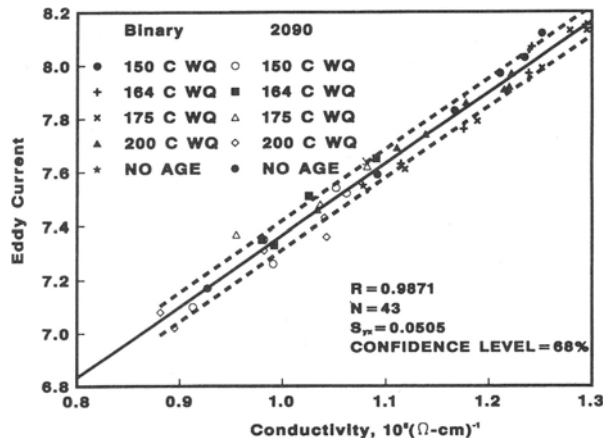


Fig. 4. Eddy current response (Al 2090 and binary alloy).

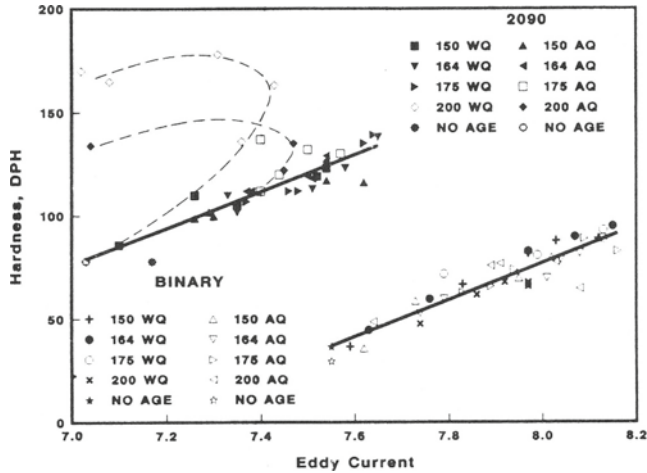


Fig. 5. Vickers hardness versus eddy current response (Al 2090 and binary).

When the eddy current response is correlated with DPH, interesting features can be observed, as seen in Fig. 5. With the exception of the Al 2090 alloy, aged at 200 C, the DPH vs. eddy current response results in a linear relationship for both the binary and the Al 2090 alloys. However note from Table I and Fig. 5 that while the slope of the linear regression lines are essentially the same, there is a significant offset. This is most likely due to the different precipitate phases present in the two alloys.

More importantly, the 200 C aging treatment of Al 2090 leads to a very unexpected result, shown in Figs. 5 and 6. In Fig. 6, both the DC conductivity and the eddy current response of water quenched Al 2090 are plotted vs. DPH revealing a nonlinear behavior of the alloy aged at 200 C. Similar results were found for air quenched Al 2090, as shown in Fig. 5. To understand the cause of this nonlinearity, three samples were chosen for TEM<sup>[7]</sup>, as listed in Table II. The selected samples are designated as A, B, and C in Fig. 6. A summary of the TEM results is given in Table II, demonstrating that the effect is obviously caused by the presence of the T<sub>1</sub> phase in sample C which is accompanied by large strains<sup>[7]</sup>.

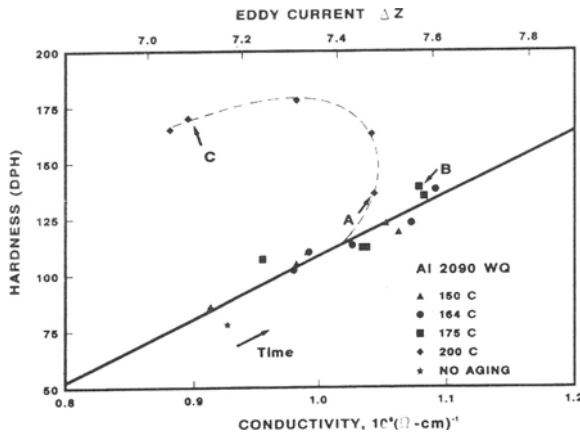


Fig. 6. Vickers hardness versus DC conductivity/eddy current response (Al 2090).

Ultrasonic measurements at 10 MHz were used to determine the sound velocity from which the elastic modulus,  $E$ , was calculated. As listed in Table I,  $E$  was found to be a constant for a constant Li concentration, independent of the aging treatment. Attenuation was calculated from the pulse-echo decay at 10 MHz. The present results indicate no systematic trends with aging treatments.

Table II. Transmission Electron Microscopy results for Al 2090.

Sample	Aging Treatment	Phases Observed
A	3 hr at 200 C	$\delta', \theta', Al_3Zr$
B	33 hr at 175 C	$\delta', \theta', Al_3Zr$
C	33 hr at 200 C	$\delta', T_1, \theta', Al_3Zr$

## DISCUSSION

This investigation has as its goal the evaluation of NDE techniques suitable to determine mechanical properties as well as precipitation processes. Statistical techniques were applied to determine correlations between mechanical properties and the NDE measurement results as well as their accuracy.

The results of the correlation of  $\sigma_y$  with DPH are quite encouraging, as indicated by a correlation coefficient of  $R=0.97$ . A single linear equation describes the correlation for both the binary and the Al 2090 alloys. Results for age hardened Al 65S, chemically similar to Al 6061, are also found to be within one standard deviation of the linear regression line. This is not surprising since all three alloys are strengthened by precipitate formation, the only difference being the composition and the morphology of the precipitates present. Since  $\sigma_y$  is determined by the onset of dislocation glide in the matrix, it is speculated that the observed correlation will also apply to other age hardened aluminum alloys such as the 2000 and 7000 series. It should also be noted that the results obtained on the binary alloy are concentrated at lower yield stresses and hardness while the Al 2090 results are at higher values. This is a result of the difference in precipitates formed as indicated by the TEM results. Thus, NDE measurements, in this case hardness, can be used to detect differences in the precipitate morphology as well as the mechanical properties.

In addition, Meyer hardness was correlated with the mechanical properties. Even though a linear correlation is evident in Fig. 2,  $R$  for this data set is considerably lower than for  $\sigma_y$  vs. DPH. This is the result of a larger scatter in the Meyer hardness results. Meyer hardness is based on the projected area of an indentation from a Rockwell tester. It is believed that the scatter is the result of differences in surface condition and inaccuracies in determining the diameter of the indentation. A more extensive evaluation is now underway.

Ultimate tensile stress,  $\sigma_{UTS}$ , is also a mechanical property of interest to the designers. Therefore, a NDE method to determine  $\sigma_{UTS}$  will be useful. With this in mind, correlations between  $\sigma_{UTS}$  and DPH were attempted. Unlike the case of  $\sigma_Y$  versus DPH, there is not a unique correlation for both the binary and Al 2090 alloys. In contrast to  $\sigma_Y$  there is usually very little change in  $\sigma_{UTS}$  with aging for a given alloy. The reason is that  $\sigma_{UTS}$  is determined not only by the precipitate morphology but also by the degree of deformation accumulated at  $\sigma_{UTS}$ . It may be possible to estimate  $\sigma_{UTS}$  using a relation proposed by Tabor<sup>[8]</sup> and Cahoon, et al.<sup>[4]</sup> based on DPH and the Meyer exponent,  $m$ . This work is also in progress.

Conductivity measurements have the advantage of being fast which make them ideal candidates for production floor NDE. A linear correlation was found for both the binary and Al 2090 with an extremely high R of 0.99. This indicates that the DC conductivity can be estimated from the simpler eddy current measurement. Certainly, the parameters in the given correlation depend on the particular probe used. In other words, the correlation given in Table I is specific to the present eddy current probe; yet once the linear equation is determined for a given probe, the conductivity can be easily estimated.

In general, the DC conductivity of an alloy increases as precipitates form because the matrix is depleted of solute atoms. The solute atoms act as electron scatterers and as the number of scatterers decreases, the conductivity increases<sup>[9]</sup>. This trend is found in both the binary and the Al 2090. The aged samples have a higher conductivity than those that have not been aged. In other words, precipitation of second phases increases the conductivity.

The DC conductivity and thus the eddy current response is larger for the binary than for the Al 2090 alloy. This mainly results from the presence of Cu in Al 2090. It is interesting to note that the slope of the linear regression line for the DPH vs. eddy current response is essentially the same although for a given eddy current response Al 2090 has a higher hardness than the binary. This indicates the slope must be related to  $\delta'$  precipitation since it occurs in both the Al 2090 and the binary alloy. The increase in hardness and yield stress for Al 2090 is a result of the Cu precipitate phases, i.e.,  $\theta'$  and  $T_1$  <sup>[10]</sup> while the binary alloy is strengthened only by the  $\delta'$  phase, as discussed earlier.

A nonlinearity in DPH versus conductivity was observed on the Al 2090 alloy, aged at 200 C. Fig. 6 shows both eddy current response and DC conductivity versus DPH for the 2090 WQ alloy. To understand the cause of this decrease in conductivity with aging time, TEM was performed on samples A, B, and C as shown in Table II<sup>[7]</sup>. Note that the  $T_1$  phase was evident after aging at 200 C for 33h but not after a 175 C treatment. This indicates that the  $T_1$  phase is responsible for the nonlinearity of the DC conductivity or eddy current response vs. DPH. Although  $T_1$  has been found to increase strength<sup>[10]</sup>, it also has a detrimental effect on fatigue properties<sup>[10,11]</sup>. For this reason,  $T_1$  is a phase to be avoided. Thus, an NDE technique that indicates its presence would be valuable. Apparently, the ideal technique is a combination of eddy current or DC conductivity versus DPH, indicated by a higher DPH than expected from the linear correlation evident for aging treatments at 175 C or below.

Ultrasonic measurements were made to determine the sound velocity and attenuation using pulse overlap techniques. The sound velocity was used to calculate the Young's modulus,  $E$ , which was found to be constant for a constant Li concentration regardless of the aging treatment. Attenuation measurements revealed no systematic trends with aging treatment for both the binary and Al 2090 alloys. However, the overall attenuation was lower in the Al 2090 alloy than in the binary. Indications are that this difference is related mainly to the Cu addition in Al 2090 providing stronger dislocation pinning and thus lower attenuation than in the binary alloy.

## CONCLUSIONS

1. Correlation of  $\sigma_y$  with hardness indicates that a single relationship describes both the binary and Al 2090 alloys. Al 65S (compositionally similar to Al 6061) results are also within one standard deviation of the linear regression line. Hardness qualitatively indicates differences in precipitation. Meyer hardness results ( $R=0.81$ ) show more scatter than Vickers hardness ( $R=0.98$ ).
2. Correlation of  $\sigma_{UTS}$  with DPH require separate relations for the binary and the Al 2090 alloys.
3. A linear relation was found between eddy current response and DC conductivity indicating that conductivity can be estimated from simpler eddy current measurements.
4.  $T_1$ , which is detrimental to fatigue properties can be detected using a combination of eddy current or DC conductivity and hardness measurements.
5. The elastic modulus was found to be constant for a constant Li concentration.
6. No systematic trends with aging treatment were found in the attenuation for either alloy.

## ACKNOWLEDGMENT

The work was sponsored by the Center for NDE at Iowa State University and was performed at the Ames Laboratory. Ames Laboratory is operated for the U.S. Department of Energy by Iowa State University under Contract No. W-7405-ENG-82.

## REFERENCES

1. The authors appreciate several pieces of Al 2090, received courtesy of R. J. Bucci and R. Westerland, Alcoa.
2. D. J. Bracci, P. Garikepati, D. C. Jiles, and O. Buck, in Review of Progress in Quantitative NDE, Vol. 7B, D. O. Thompson and D. E. Chimenti, Eds., Plenum Press, New York and London, 1255 (1988).
3. G. W. Snedecor, W. G. Cochran, Statistical Methods, Iowa State University Press, Ames, Iowa (1967).
4. J. R. Cahoon, W. H. Broughton and A. R. Kutzak, *Met. Trans.* **2**, 1979 (1971).
5. W. F. Smith, Structure and Properties of Engineering Alloys, McGraw Hill, New York (1981).
6. G. E. Dieter, Mechanical Metallurgy, McGraw Hill, New York (1986).
7. O. Buck, L. J. H. Brasche, J. E. Shield, D. J. Bracci, D. C. Jiles and L. S. Chumbley, "Nondestructive Detection of the  $T_1$  phase in Al-Li Alloys", submitted to *Scripta Met.*
8. D. Tabor, *J. Inst. Met.*, **79**, 1 (1951).
9. W. D. Rummel, *Mat. Eval.*, **24**, 507 (1966).
10. K. V. Jata and E. A. Starke, in "Aluminum-Lithium Alloys III", C. Baker, P. J. Peel, Eds., The Institute of Metals, London, 247 (1986).
11. M. R. James, *Scripta Met.*, **21**, 783 (1987).